SEISMIC BEDROCK DEPTH MEASUREMENTS AND THE ORIGIN OF GEORGE VI SOUND, ANTARCTIC PENINSULA

M. P. MASLANYJ

British Antarctic Survey, Natural Environment Research Council, High Cross, Madingley Road, Cambridge CB3 0ET, UK

ABSTRACT. Seismic sounding has been used to determine bedrock depths beneath George VI Ice Shelf. A contour map and profiles illustrate the bedrock topography. The ice shelf is underlain by a deep steep-sided elongated trough trending N–S in the north and E–W in the south with bedrock depths exceeding 800 and 1000 m respectively. This supports the concept that George VI Sound is, in part, an extensional feature. Hydrographic soundings suggest that the rift-like feature extends north to at least lat. 68° 30′ S. The present setting of Alexander Island is explained in terms of crustal extension producing north-westwards movement relative to the Antarctic Peninsula. In southern George VI Sound rifting developed sub-parallel to the continental margin whereas in the north it formed discordantly to the margin and possibly along an older tectonic boundary. It is not possible to relate the opening to a particular episode of extension due to limited age constraints, and the present configuration is a consequence of as yet undefined geological processes complicated by subsequent glacial modification.

INTRODUCTION

George VI Sound is a linear geomorphological feature on the west coast of the Antarctic Peninsula, separating Alexander Island from Palmer Land (Fig. 1). It is a channel 500 km in length with a width of 30 km in the north widening to over 70 km in the south. Over most of its length it is covered by George VI Ice Shelf through which depths to seabed of over 1000 m have been recorded (Crabtree and others, 1985).

George VI Sound forms a major divide between the Mesozoic sediments of Alexander Island and the Lower Jurassic–Cretaceous magmatic arc-related rocks of the Antarctic Peninsula. The origin of Alexander Island is disputed. Storey and Garrett (1985) propose a model in which George VI Sound is considered to be a region of intra-arc extension displacing *in situ* accretionary prism and fore-arc sediments from magmatic arc rocks, the boundary marking the line of an older Mesozoic fore-arc. Conversely Taylor and Shaw (1985) use palaeomagnetic evidence to suggest that Alexander Island represents a displaced terrane derived from lower latitudes.

George VI Sound is considered a rift (King, 1964; Bell, 1975; Storey and Garrett, 1985). However, its structure, age and tectonic setting are not fully understood. The northern end of the sound displays features typical of a rift valley including parallel coastlines, linear mountain ranges, and a pronounced topographic relief related to uplift (King, 1964). Near the eastern coast of northern Alexander Island, the bedrock reaches heights of 400 m above sea level and a few kilometres further inland heights exceed 1000 m. Over northern Palmer Land heights of 500 m are recorded within 5 km of the coast. South of the Batterbee Mountains, George VI Sound widens and there is a change from a NNW–SSE to an E–W orientation. There is no evidence indicating whether the southern part is a rifted basin or a simple graben. Crabtree and others (1985) have explained the widening as due to block faulting in the Goodenough Glacier area, where depths to bedrock exceed 1000 m below sea level.

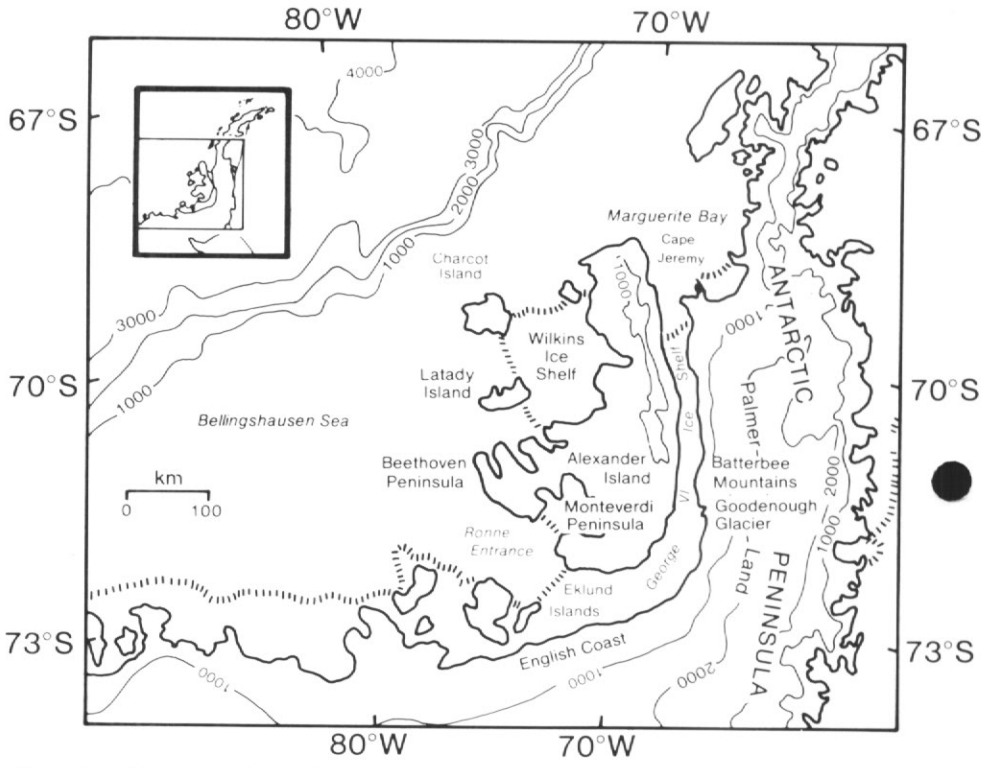

Fig. 1. Location map and general physiography of George VI Sound. (Elevations and depths in metres.)

The parallel mountain ranges observed in the north are absent, and the topography of the region is altogether more subdued.

George VI Sound probably forms part of a more extensive rift system. The eastern coastline of the sound coincides with the western edge of a batholithic body reflected by the West Coast Magnetic Anomaly (WCMA) (Renner and others, 1985). Crabtree and others (1985) described two major N–S trending fault zones in Palmer Land, the one to the east probably representing the eastern boundary of the rift system. Aeromagnetic evidence (Renner and others, 1985) indicates that the western coastline of George VI Sound may not form a distinct geological boundary. Butler (19[illegible]) recognized a linear Bouguer anomaly extending in a N–S direction, almost parallel to George VI Sound in central Alexander Island and this is thought to be associated with block faulting. Edwards (1979) considered the possibility that sub-parallel faulting in central Alexander Island is related to rifting, and suggested that the LeMay Range fault may be the true western edge of the rift. By contrast, evidence of rifting and parallel faulting in south-east Alexander Island is minimal (Horne, 1967). The northern and southern extremes of the rift zone remain uncertain.

Direct evidence for the age of rifting has not been found. Field relations (BAS Geological Map, 1981) indicate that the youngest rocks displaced are of Albian age (113–97 Ma). Tertiary calc-alkaline volcanic rocks dated at 60–40 Ma (Burn, 1981) are thought to be bounded by N–S trending faults in northern Alexander Island. Post rift rocks are probably represented by minor amounts of alkaline volcanics dated at 7–5 Ma (R. J. Pankhurst, pers. comm. 1986).

In this paper, seismic depths to bedrock and recent bathymetric soundings are presented with a view to defining more closely the morphology and extent of George VI Sound. The geological implications are discussed.

Field Technique

Following two exploratory traverses during November and December 1983, seismic depth-to-bedrock and short refraction surveys were completed between December 1984 and February 1985 as part of a regional gravity investigation. Traverses were run perpendicular to the regional structural trend of George VI Sound with seismic measurements every 3 km in the north and every 4 km in the south. The work of Crabtree and others (1985) indicates that this spacing was detailed enough for the identification of significant sub-ice topographic and structural features. Station coordinates were determined by Magnavox 4102 satellite navigation equipment supplemented by resection to identifiable topographic features.

Seismic depth to bedrock survey

A Nimbus ES1210F 12-channel signal-enhancement seismograph was used. Geophones were arranged at 30 m intervals along a 380 m in-line spread with a 50 m shot point offset. The unreversed spread was normally extended along the direction of the traverse, preferably down the dip of the underlying bedrock. The energy source was 0.45 kg of Seismex High Explosive with the same quantity of Seismex Primer. Shot-holes were drilled either by a Jiffy ice drill or by a hand ice-corer and were typically 4–5 m deep although this varied according to the snow surface encountered. Two shots were usually fired at each site.

A total of 101 seismic stations were occupied. At each station the first record was normally over a long period (1000 ms record 200 ms delay) and was used to identify the sea-bottom reflection ($I_1 W_1$). Strong reflections observed on George VI Ice Shelf included those generated at the ice–water interface (I_1), multiples (e.g. I_2, $I_2 W_1$, etc.) and $S \rightarrow P$ wave conversions at this boundary. The second record with a predetermined 200 ms interval was then used to define more accurately the arrival time of the $I_1 W_1$ event (the *in situ* assessment of radio-echo sounding and gravity information from previous sites often allowed the prediction of the arrival time, resulting in only one record being required at some stations). Most records incorporated a high pass 80 Hz filter to reduce persistent low-frequency, shot-generated surface noise.

Short seismic refraction survey

The short seismic refraction survey was necessary to determine the velocity of propagation of longitudinal P waves in the near surface layer of ice to provide velocity control for the reflection events.

Normally two short refraction sites were established on each traverse. At each, an unreversed profile was obtained along the line of the traverse, the seismic energy being generated by a series of hammer blows on a coupling plate. The arrival times were recorded using 22 geophones on two separate records. The geophones for the first record were at 2.5, 5, 7.5, 10, 15, 20, 30, 40, 50, 60, 70 and 80 m, and to observe the deeper refracted waves on the second, at 30 m intervals between 50–380 m.

Radio-echo ice thickness survey

Two hundred and ten radio-echo sounding measurements were made on the ice shelf using a sledge-towed 60 MHz ice-sounding radar. The values were used to determine surface elevations for the gravity stations, and for calculating the absolute bedrock depths from the seismic reflection records.

Radio-echo sounding techniques are generally preferred to seismic reflection methods for ice thickness measurements on ice shelves because the ice–water interface is not usually identifiable from seismic records. However, George VI Ice Shelf proved unusual in this respect in providing a good seismic ice–water return which can probably be attributed to the strong bottom melting described by Bishop and Walton (1981).

Data Analysis

Determination of bedrock depth

Bedrock depths are calculated from the total travel time (T_t) of the $I_1 W_1$ seismic reflections. Generally these were strong and could be measured to ± 0.5 ms. The less easily identifiable $I_1 W_1$ returns give errors of ± 10 ms.

The total P wave travel time T_t is given by:

$$T_t = T_I + T_W, \tag{1}$$

where T_I is the two-way travel time in ice and T_W is the two-way travel time in sea water.

Assuming a P wave velocity of 1.445 km s^{-1} in sea water, and provided that the travel time in the ice shelf can be accurately measured, the depth to bedrock can be determined. The two-way travel time in ice is given by:

$$T_I = 2\left(\frac{I-S}{V_{ice}}\right) + T_s \tag{2}$$

where I is the ice shelf thickness (in metres) determined by radio-echo sounding; V_{ice} is the velocity of P waves in ice (3.86 km s^{-1}); and T_s is the travel time of P waves in the upper S metres of the ice sheet.

T_s (due to the lower velocity P waves in the firn) is determined from the refraction record; the first arrival is picked to the nearest 0.5 ms for the various offsets and a time–distance curve used to determine velocities as a function of distance. Velocities as a function of depth are then determined using the standard integral formula of Wiechart, Herglotz and Bateman (Slichter, 1932),

$$Z_{x_1} = \frac{1}{\pi}\int_0^{x_1} \cosh^{-1}\left(\frac{V_{x_1}}{V_x}\right) dx, \tag{3}$$

where Z_{x_1} is the depth corresponding to velocity V_{x_1}. This gives the maximum depth penetrated by the refracted wave first received at distance x_1 (the formula is valid provided that there is no decrease in velocity with depth). Examples of the velocity–depth curves for sites on George VI Ice Shelf are shown in Fig. 2. The near-surface velocity distribution is also used in calculating the shot depth correction incorporated in the total travel time. The ice shelf surface was considered sufficiently level that corrections for variations in geophone heights were not required.

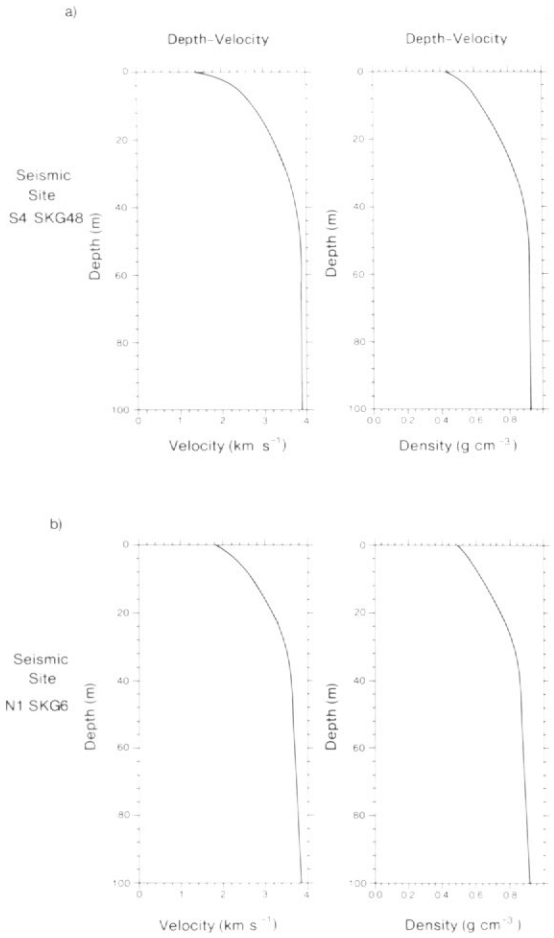

Fig. 2. Velocity–depth and density–depth curves for (a) seismic site S4 SKG 48, southern George VI Sound; (b) Seismic site NI SKG 6, northern George VI Sound.

Density determination using short seismic-refraction profiles

To determine bedrock depth below sea level it is necessary to determine the absolute height of the ice shelf surface. The elevation can be derived from hydrostatic principles using ice shelf thickness and density measurements. The method of density determination is based on an empirical equation (Kohnen, 1972) converting the seismic velocity–depth function to an ice density–depth function:

$$\rho(z) = 0.915\left[1+\left\{\frac{V_{\text{ice}}-V(z)}{2.25\ \text{m s}^{-1}}\right\}^{1.22}\right]^{-1}\ \text{Mg m}^{-3}. \quad (4)$$

Using refraction profiles from the Greenland and Antarctic ice sheets, Kohnen (1971) found that above the firn line the velocities of seismic waves in the ice increase monotonically with increasing depths. The maximum depth of penetration of the refracted waves corresponds to a depth where the densification rate is negligible.

The method has been used on the Ross Ice Shelf (Kirchner and Bentley, 1979) and on the Ronne Ice Shelf where Herrod and Garrett (1986) calculated the density profile

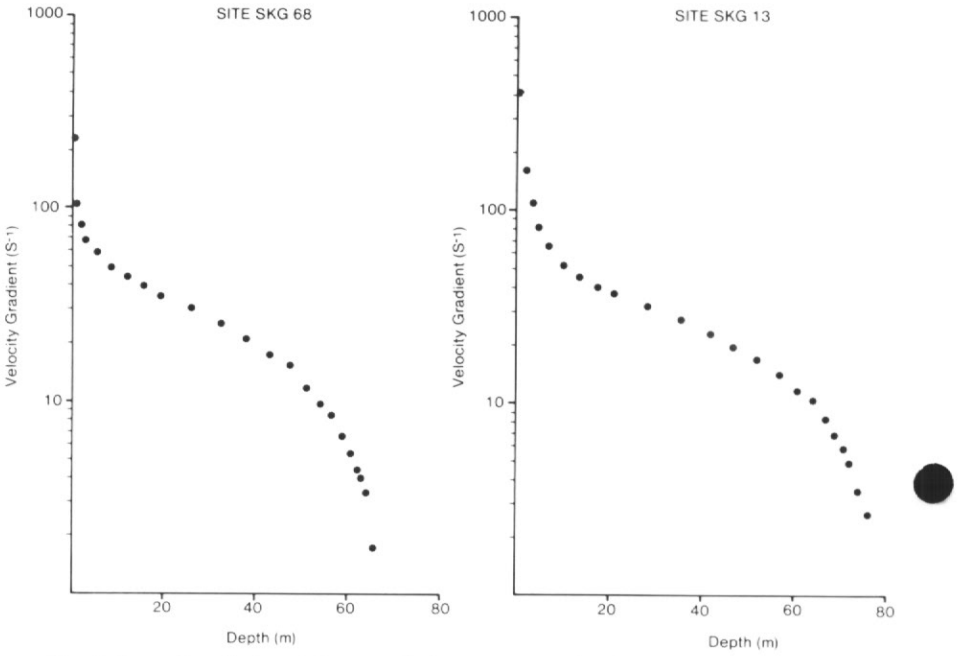

Fig. 3. Examples of selected *P* wave velocity gradient *vs.* depth curves on George VI Sound.

to a depth of 100 m, the deeper ice being assumed to have a maximum density approaching 0.917 Mg m^{-3}. However, George VI Ice Shelf is subject to annual permeation and refreezing of melt water which may affect the accuracy of this method by: (1) High density surface layers reducing the depth of penetration of the seismic waves; (2) A possible hidden layer effect due to decrease in density with depth.

Despite the limitations, the determined curves of velocity gradient *vs.* depth (Fig. 3) are similar to those given by Bentley (1975); the inflexions in slope are thought to represent critical densification horizons. The technique provides an average density over the length of the geophone spread and thus avoids any local variations which might otherwise bias coring measurements. The density–depth curves (Fig. 2) indicate a near surface density of approximately 0.4 Mg m^{-3} which then generally increases rapidly within the upper 50 m to 0.9 Mg m^{-3}. Density determinations for various locations are presented in Table I. Values for intermediate sites are obtained assuming that the density changes linearly between the limits determined at the refraction sites. Estimates of density on the ice shelf by Doake (1984) and Bishop and Walton (1981) broadly conform to those given in Table I.

The error in the density using the seismic refraction method is considered to be ± 0.01 Mg m^{-3}. Combined with an error of ± 10 m in the RES ice thickness this results in seismic bedrock depth errors of ± 5 to ± 10 m over the length of George VI Sound. The calculation does not include the effect of temperature and anisotropy, which Kohnen (1974) has estimated at < 0.01 Mg m^{-3} for continental ice sheets.

Over the grounded ice of George VI Sound, Wallace and Tierman altimeters were used to determine heights.

Table I. Density values determined from the seismic refraction survey. George VI Ice Shelf.

Seismic site	*Lat.* (*S*)	*Long.* (*W*)	*Max depth of refracted* P *wave* (*m*)	*Ice shelf thickness* (*RES*) (*m*)	*Average density to depth of* 100 *m* ($Mg\ m^{-3}$)	*Average density of ice shelf* ($Mg\ m^{-3}$)
N1 SKG 1	70° 15.22′	68° 50.18′	47	127	0.80	0.87
N1 SKG 6	70° 15.07′	68° 25.83′	49	140	0.82	0.88
S2 SKG 13	72° 35.67′	67° 43.17′	78	370	0.79	0.88
S2 SKG 24	72° 21.46′	68° 41.29′	25	341	0.84	0.89
S4 SKG 45	72° 14.67′	67° 28.23′	86	382	0.74	0.87
S4 SKG 82	72° 16.80′	67° 05.78′	55	412	0.82	0.89
S5 SKG 62	72° 38.04′	69° 33.23′	28	440	0.82	0.89
S6 SKG 68	72° 47.17′	70° 36.41′	66	414	0.79	0.89
S6 SKG 76	73° 03.93′	70° 53.37′	83	301	0.79	0.88

Table II. Radio-echo ice thickness and seismic reflection bedrock depths along George VI Sound.

Traverse	*Site*	*Position*		*Ice thickness* (*m*)	*Bedrock depth below sea level* (*m*)
		Lat. (*S*)	*Long.* (*W*)		
N1	SKG 1	70° 15.22′	68° 50.18′	127	611
Mount Alfred–	SKG 2	70° 15.21′	68° 45.13′	125	486
Carse Point	SKG 3	70° 15.19′	68° 40.32′	140	466
	SKG 4	70° 15.12′	68° 35.34′	150	486
	SKG 5	70° 15.25′	68° 30.62′	145	561
	SKG 6	70° 15.07′	68° 25.83′	140	656
	SKG 7	70° 14.96′	68° 20.99′	136	518
	SKG 8	70° 14.91′	68° 15.82′	150	637
N2	SKG 9	70° 30.23′	67° 55.9′	93	397
Moore Point–	SKG 10	70° 30.17′	68° 00.83′	124	630
Calf Point	SKG 11	70° 30.38′	68° 05.92′	152	689
	SKG 12	70° 30.56′	68° 11.05′	168	740
	SKG 13	70° 30.73′	68° 15.67′	163	553
	SKG 14	70° 30.98′	68° 20.48′	170	653
	SKG 15	70° 31.13′	68° 25.23′	171	418
	SKG 16	70° 31.33′	68° 30.34′	128	355
N3	SKG 17	70° 38.36′	68° 23.87′	116	280
Belemnite	SKG 18	70° 39.04′	68° 19.08′	133	406
Point–	SKG 19	70° 39.67′	68° 14.29′	139	495
Wade Point	SKG 20	70° 40.43′	68° 08.63′	144	620
	SKG 21	70° 40.98′	68° 04.21′	156	639
	SKG 22	70° 41.42′	67° 59.39′	159	787
	SKG 23	70° 42.36′	67° 54.43′	148	903
	SKG 24	70° 42.88′	67° 49.48′	149	786
N4	SKG 6	71° 20.97′	67° 43.50′	230	729
Fossil Bluff–	SKG 7	71° 21.18′	67° 38.38′	243	460
Batterbee	SKG 8	71° 20.71′	67° 49.06′	226	826
Mountains	SKG 9	71° 20.06′	67° 52.36′	209	777
	SKG 10	71° 20.32′	67° 54.39′	193	699
	SKG 11	71° 19.78′	68° 05.90′	180	611
	SKG 12	71° 19.57′	68° 11.44′	177	799
S2	SKG 13	72° 35.67′	67° 43.17′	370	830
Kirwan	SKG 14	72° 37.19′	67° 37.53′	387	822
Inlet	SKG 15	72° 34.28′	67° 48.94′	395	840
	SKG 16	72° 32.80′	67° 54.57′	378	757
	SKG 17	72° 31.41′	68° 00.89′	378	770
	SKG 18	72° 30.00′	68° 06.78′	378	762
	SKG 19	72° 28.54′	68° 12.55′	370	719
	SKG 20	72° 27.19′	68° 18.39′	362	594
	SKG 21	72° 25.76′	68° 24.14′	362	507
	SKG 22	72° 24.64′	68° 30.38′	357	484
	SKG 23	72° 22.86′	68° 35.62′	362	508
	SKG 24	72° 21.46′	68° 41.29′	341	438
	SKG 25	72° 20.05′	68° 47.01′	349	426
S3	SKG 25	71° 52.90′	67° 07.04′	284	544
Northern	SKG 26	71° 53.92′	67° 13.35′	299	775
Goodenough	SKG 27	71° 54.93′	67° 19.89′	317	1006
Glacier–	SKG 28	71° 55.95′	67° 26.46′	353	932
Coal Nunatak	SKG 29	71° 56.97′	67° 32.97′	340	876
	SKG 30	71° 57.89′	67° 39.40′	337	763
	SKG 31	71° 58.08′	67° 47.00′	320	618
	SKG 32	71° 59.79′	67° 52.43′	308	439
	SKG 33	72° 00.71′	67° 58.67′	299	537
	SKG 34	72° 01.91′	68° 05.15′	316	584

Table II. (cont.)

Traverse	Site	Position		Ice thickness (m)	Bedrock depth below sea level (m)
		Lat. (S)	Long. (W)		
	SKG 35	72° 02.73′	68° 11.74′	297	501
	SKG 36	72° 03.69′	68° 18.44′	284	365
S4	SKG 37	72° 09.37′	68° 15.79′	345	486
Titan	SKG 38	72° 08.69′	68° 22.48′	309	306
Nunatak–	SKG 39	72° 10.25′	68° 08.84′	342	427
Buttress	SKG 40	72° 11.04′	68° 01.88′	324	457
Nunataks	SKG 41	72° 11.80′	67° 55.34′	359	511
	SKG 42	72° 12.51′	67° 48.50′	366	757
	SKG 43	72° 13.24′	67° 41.97′	416	936
	SKG 44	72° 13.92′	67° 35.17′	409	940
	SKG 45	72° 14.67′	67° 28.23′	382	965
	SKG 46	72° 15.34′	67° 21.64′	371	946
	SKG 47	72° 16.02′	67° 14.70′	376	973
	SKG 48	72° 16.60′	67° 07.82′	376	679
	SKG 49	72° 17.29′	67° 01.00′	455	760
S5	SKG 51	72° 58.83′	68° 38.85′	427	461
Eastern	SKG 50	72° 56.89′	68° 43.73′	442	735
English coast–	SKG 52	72° 55.26′	68° 49.01′	466	764
southern	SKG 53	72° 53.10′	68° 52.14′	465	842
Alexander	SKG 54	72° 51.76′	68° 57.39′	468	978
Island	SKG 55	72° 50.10′	69° 02.23′	490	966
	SKG 56	72° 48.33′	69° 06.53′	499	903
	SKG 57	72° 46.71′	69° 11.30′	474	882
	SKG 58	72° 44.97′	69° 15.86′	476	743
	SKG 59	72° 43.23′	69° 20.45′	409	642
	SKG 60	72° 41.25′	69° 25.69′	420	572
	SKG 61	72° 39.85′	69° 29.33′	459	539
	SKG 62	72° 38.04′	69° 33.23′	440	478
	SKG 63	72° 36.27′	69° 37.43′	505	440
S6	SKG 67	72° 40.26′	70° 19.47′	356	577
Southern	SKG 66	72° 41.86′	70° 24.69′	324	654
Alexander	SKG 65	72° 43.25′	70° 27.19′	343	542
Island–	SKG 64	72° 45.08′	70° 34.12′	370	578
east of	SKG 68	72° 47.17′	70° 36.41′	414	849
Eklund	SKG 69	72° 49.48′	70° 38.76′	422	894
Islands	SKG 70	72° 51.58′	70° 40.41′	446	1045
	SKG 71	72° 53.01′	70° 43.00′	465	1066
	SKG 72	72° 55.51′	70° 44.76′	472	841
	SKG 73	72° 57.60′	70° 46.87′	414	817
	SKG 74	72° 57.12′	70° 48.82′	349	688
	SKG 75	73° 01.83′	70° 51.20′	307	492
	SKG 76	73° 03.93′	70° 53.37′	301	420
	SKG 77	73° 06.08′	70° 54.62′	382	557
	SKG 78	73° 08.23′	70° 54.77′	314	531
	SKG 79	73° 09.79′	70° 52.22′	239	652
	SKG 80	73° 12.36′	70° 50.37′	197	558
	SKG 81	73° 14.37′	70° 47.61′	291	540

Results

Ice thickness and bedrock depths are given in Table II and presented as profiles and a contour map in Fig. 4. Additional bedrock depths incorporated in the map include weighted-line measurements, a 40 km seismic reflection profile (Crabtree and

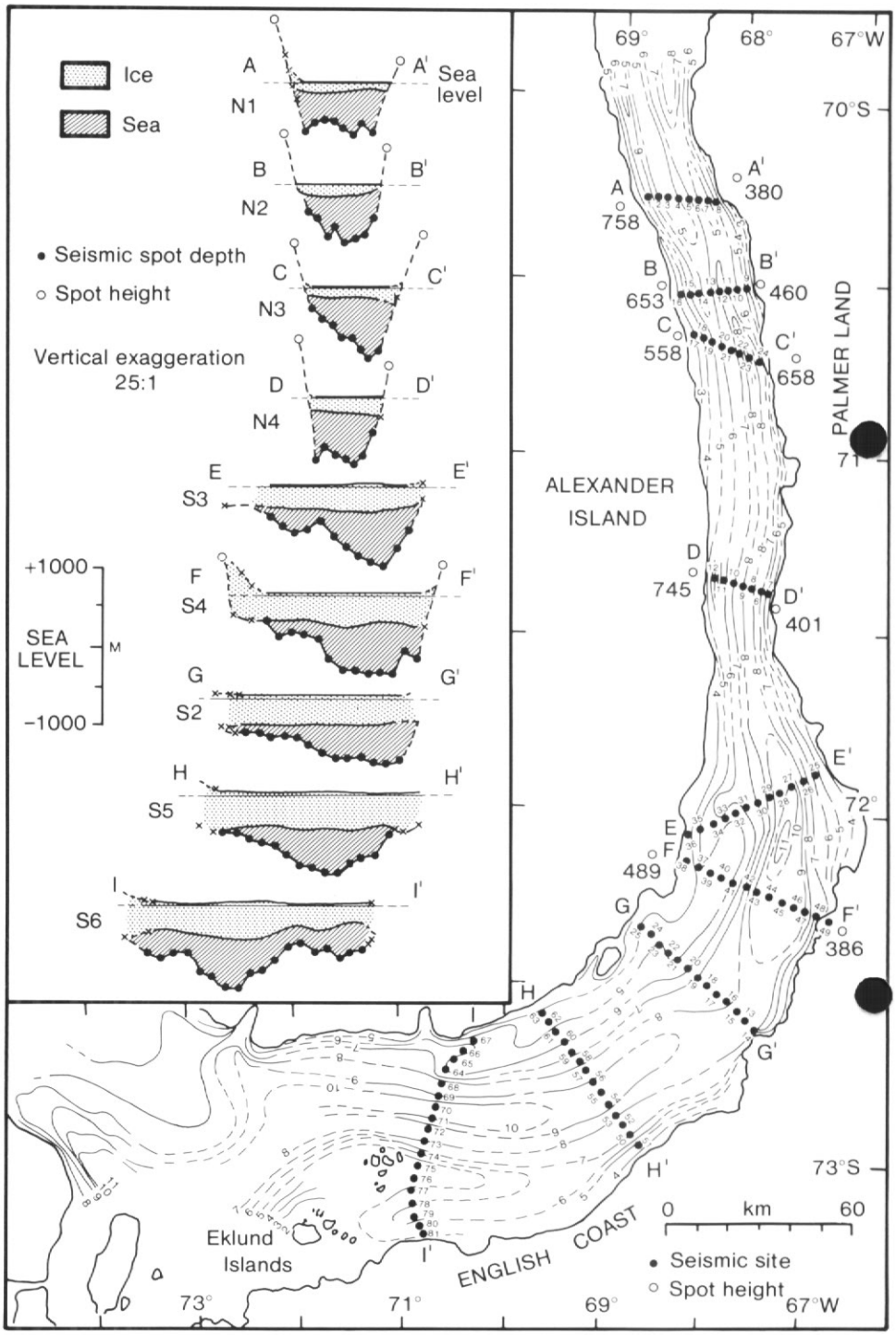

Fig. 4. Profiles of ice thickness and bedrock depths below sea level and bathymetric contour map of George VI Sound (contour interval 100 m).

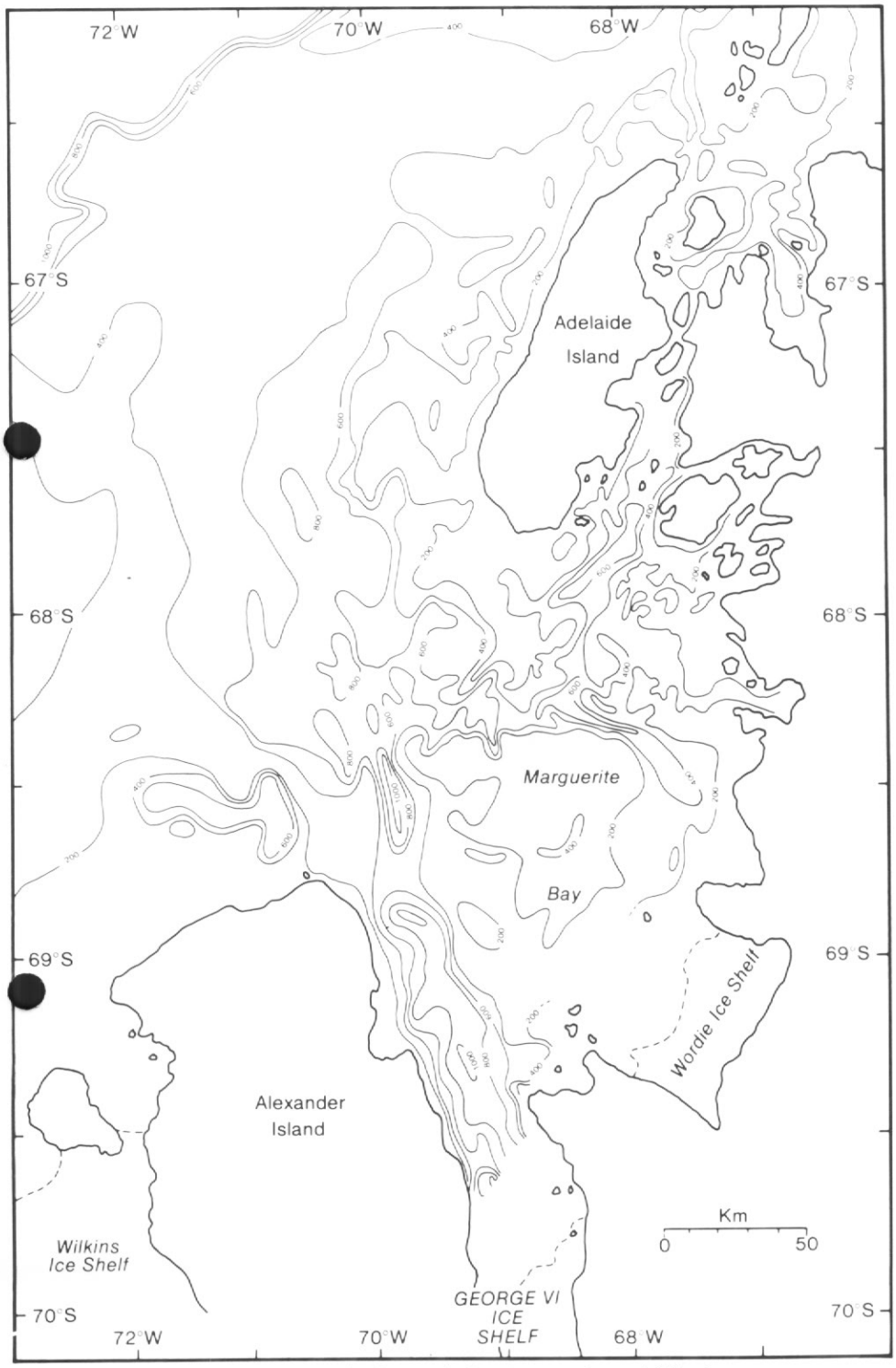

Fig. 5. Bathymetry in Marguerite Bay (contour interval 200 m).

others, 1985), and bathymetric soundings taken by RRS *Bransfield* in the Ronne Entrance (1984–85). To extend the profiles inland, available surface elevations and ice thicknesses obtained from airborne radio-echo sounding have been incorporated.

The contouring is governed by the data distribution but significant features are:

(1) George VI Sound is underlain by a deep elongated trough.

(2) The bathymetric character of George VI Sound changes along its length. In the north a deep trough runs parallel to the coastlines with a recorded maximum depth of over 900 m near Wade Point (Fig. 4 profile N3). South of the Batterbee Mountains (Fig. 1) where the sound is significantly wider, the sub-ice topography is typified by deeper (> 1000 m) and broader features, although the steep flanking walls are still prominent (e.g. southern Alexander Island and the English Coast).

(3) The W-shaped cross-section identified in George VI Sound by Crabtree and others (1985) is not apparent along its entire length. For instance profile N1 exhibits a more irregular sea-bottom and profile N3 shows only progressive deepening towards the Antarctic Peninsula mainland. Where it is observed (e.g. profiles N2, N4, S3) there is a marked asymmetry, with a narrow western limb and a more open, deeper eastern limb. The asymmetry becomes more pronounced to the south, where the eastern limb broadens and the western limb diminishes (profiles S2 and S5).

(4) In the central section of George VI Sound the bedrock topography suggests a change in structural trend. Profiles S2, S5 and S6 indicate a prominent NE–SW trough which becomes E–W trending as it extends towards the Ronne Entrance. Conversely, profiles S3 and S4 indicate a N–S elongated trough which is a continuation of the deep eastern limb represented on the northern profiles.

(5) Beneath George VI Sound are local bedrock highs which cannot be correlated across adjacent profiles. At the Eklund Islands a system of ice rises is seen at the surface, close to an area of bedrock shoaling to the east (profile S6).

Hydrographic soundings (Admiralty Chart 3571, including the additional soundings of HMS *Endurance* in 1985–86) in Marguerite Bay are presented as a contour map in Fig. 5. Although the area exhibits complicated bathymetry, a deep water channel extends for at least 200 km north of George VI Ice Shelf. The northerly extent of the channel is interrupted at lat. 68° 30′ S by an E–W bathymetric feature. Further to the north a 500 m channel can be recognized on the Tectonic map of the Scotia arc (1985) eventually converging with and appearing to offset the continental slope at lat. 66° 30′ S. However, this is not as deep as the trough underlying the ice shelf, nor does it exhibit the elevated limbs.

In the Ronne Entrance at the southern end of George VI Sound, hydrographic soundings indicate a seaward continuation of the trough with depths exceeding 800 m, but it is not known whether the deep water continues as far as the continental slope.

Discussion of Structural Evolution of George VI Sound

It is almost certain that George VI Sound was fully occupied by ice at glacial maxima (Crabtree and others, 1985), in which case it is likely that ice exploited a pre-existing structural line. These results indicate that the W-profile (Crabtree and others, 1985) is atypical, the bedrock topography underlying the ice shelf varying considerably between profiles. The variation may partly reflect glacial modification; if so, it is uncertain which areas represent sites of either glacial deposition or erosion. Davey (1971) described a partial infill of low density sediments, probably of glacial origin, in the deep trough underlying the Bransfield Strait. Fedorov and others (1982) recognized low density, sedimentary, graben-fill deposits in the Lambert Glacier area.

Given the possibility of glacial deposits, then, many of the depths recorded under George VI Ice Shelf do not represent structural basement, which could be significantly deeper.

The break in bathymetric contour pattern in Marguerite Bay close to the northern edge of Alexander Island could represent a structural discontinuity, the E–W trending boundary at lat. 68° 30′ S representing the termination of the sound. The 500-m deep channel which continues further to the north may be of glacial origin (Johnson and others, 1982); the outer continental shelf often exhibits similar glacial troughs (Vanney and Johnson, 1976). The possibility that the geological structure extends north to the shelf margin at lat. 66° 30′ S cannot be excluded.

The results do not bear directly on the question of the origin of Alexander Island. However, they do support the concept that George VI Sound is, in part, an extensional feature. Although the recorded depths are shallower, the sound exhibits similar topography and dimensions to inferred rifts and components of major rift zones in other parts of Antarctica (Masolov and others, 1980). The distinct E–W and N–S trending sub-ice channels also suggest that by a process of extension normal to the continental margin, Alexander Island was offset north-westwards rather than westwards (Tectonic map of the Scotia arc, 1985) relative to Palmer Land (Fig. 6). The shape of the western margin of the West Coast Magnetic Anomaly (WCMA) on the aeromagnetic anomaly map of the Antarctic Peninsula (Renner and others, 1985) suggests a similar direction of displacement (Fig. 6), which also parallels the trend of the Tula and Heezen oceanic fracture zones. Examination of Fig. 7 indicates that

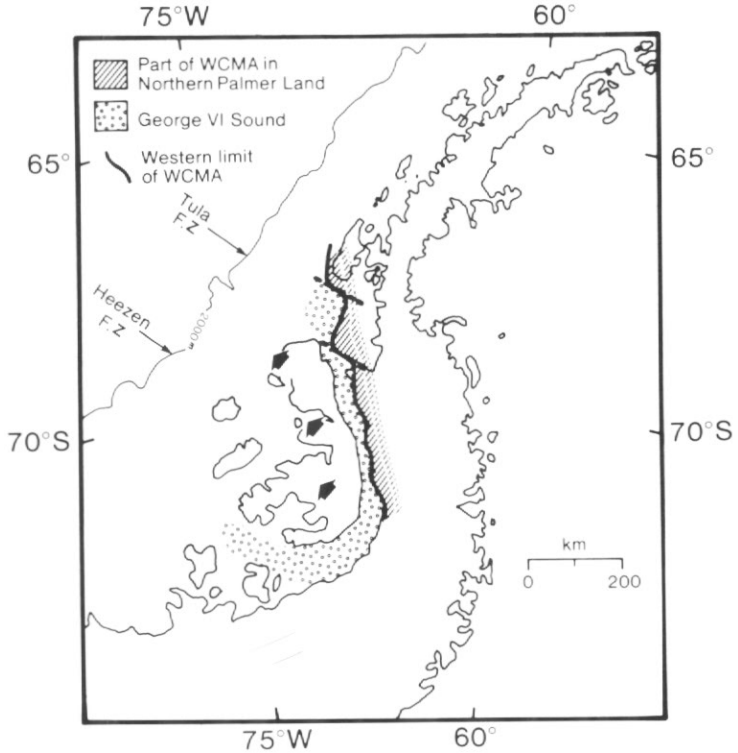

Fig. 6. North-westerly movement of Alexander Island and similar direction of displacement of the western boundary of the WCMA in northern Palmer Land.

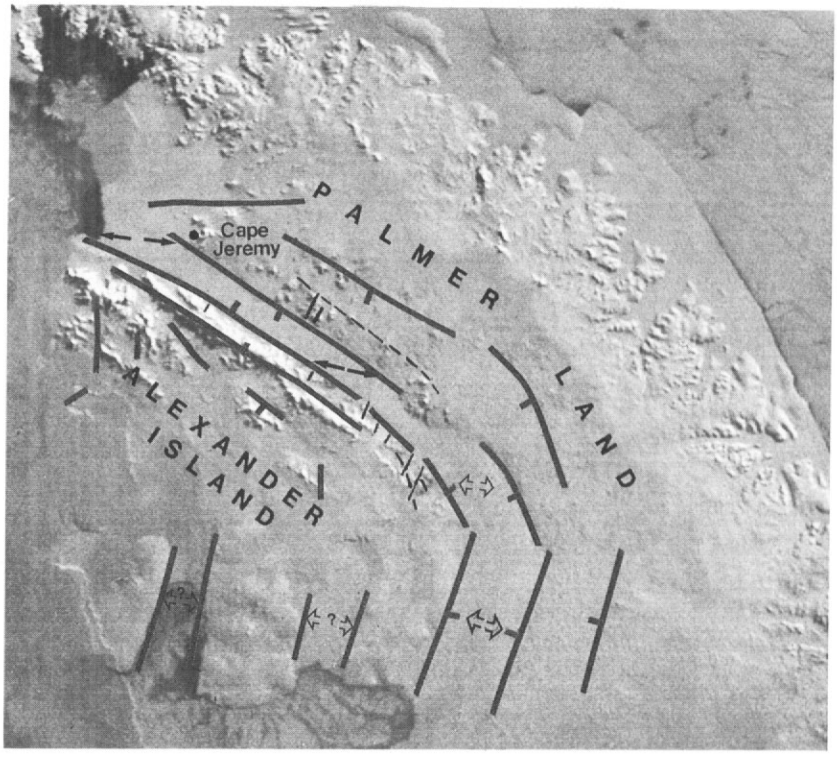

Fig. 7. Major fault boundaries, areas of subsidence and predominant extension directions superimposed on a NOAA VHRR satellite image.

a reversed (SE) movement of 90 km would realign the northern edge of Alexander Island with Cape Jeremy at lat. 69° 25′ S, would close southern George VI Sound and produce a convincing coastline fit. In the southern part, the broader and deeper topography suggests subsidence associated with regional extension. Here, the rifting developed sub-parallel to the Antarctic Peninsula continental margin (Fig. 1). The troughs separating Charcot and Latady islands, and the Beethoven and Monteverdi peninsulas are parallel to the English Coast and may be related to the same extension (Fig. 7). In the north, possibly under the influence of a palaeotectonic line, rifting developed discordantly to the margin (Fig. 1), and produced oblique movement between opposite coastlines.

Processes causing the opening of George VI Sound remain conjectural due to the limited age constraints available and the uncertainty regarding mechanisms of extension over the last 200 Ma. The present day configuration of George VI Sound represents the consequence of, as yet, undefined geological processes further complicated by subsequent glacial modification.

Acknowledgements

I wish to thank L. D. B. Herrod for advice and co-operation on the 1983–84 oversnow traverses and express my gratitude to D. A. Roberts, D. Stewart and

A. R. Simpson for their continual support and enthusiasm throughout the 1984–85 field season.

Received 18 December 1986; accepted 22 January 1987

References

BELL, C. M. 1973. Structural geology of parts of Alexander Island. *British Antarctic Survey Bulletin*, Nos. 41 and 42, 43–58.

BENTLEY, C. R. 1975. Advances in geophysical exploration of ice sheets and glaciers. *Journal of Glaciology*, **15** (73), 113–35.

BISHOP, J. F. *and* WALTON, J. L. W. 1981. Bottom melting under George VI Ice Shelf, Antarctica. *Journal of Glaciology*, **27** (97), 429–46.

BRITISH ANTARCTIC SURVEY. 1981. Geological map 1:500000, BAS 500G Sheet 4. Edition 1.

BRITISH ANTARCTIC SURVEY. 1985. Tectonic map of the Scotia arc, 1:3000000, BAS (Misc.), 3.

CRABTREE, R. D., STOREY, B. C. *and* DOAKE, C. S. M. 1985. The structural evolution of George VI Sound, Antarctic Peninsula. (*In* HUSEBYE, E. S., JOHNSON, G. L. *and* KRISTOFFERSEN, Y. *eds. Geophysics of the polar regions, Tectonophysics*, vol. 114, 431–42.)

DAVEY, F. J. 1971. Marine gravity measurements in Bransfield Strait and adjacent areas. (*In* ADIE, R. J., *ed. Antarctic geology and geophysics*. Oslo Universitetsforlaget, 39–45).

DOAKE, C. S. M. 1984. Ice-shelf densities from a comparison of radio echo and seismic soundings. *Annals of Glaciology*, **5**, 47–50.

EDWARDS, C. W. 1979. New evidence of major faulting on Alexander Island. *British Antarctic Survey Bulletin*, No. 49, 15–20.

FEDOROV, L. V., GRIKUROV, G. E., KURININ, R. G. *and* MASOLOV, V. N. 1982. Crustal structure of the Lambert Glacier area from geophysical data. (*In* CRADDOCK, C. *ed. Antarctic geoscience*. The University of Wisconsin Press, 931–7.)

HERROD, L. D. B. *and* GARRETT, S. W. 1986. Geophysical fieldwork on the Ronne Ice Shelf. *First Break*, **4**, No. 1.

HORNE, R. R. 1967. Structural geology of part of south-eastern Alexander Island. *British Antarctic Survey Bulletin*, No. 11, 1–22.

HYDROGRAPHIC DEPARTMENT. 1983. Admiralty Chart No. 3571 supplemented with soundings by HMS *Endurance* 1985–6.

JOHNSON, G. L., VANNEY, J. R. *and* HAYES, D. 1982. The Antarctic continental shelf (Review Paper). (*In* CRADDOCK, C. *ed. Antarctic geoscience*. The University of Wisconsin Press, 995–1003.)

KING, B. C. 1970. Vulcanicity and rift tectonics in East Africa. (*In* CLIFFORD, T. N. *and* GASS, I. G., *eds. African magmatism and tectonics*. Edinburgh, Oliver and Boyd, 263–83.)

KING, L. 1964. Pre-glacial geomorphology of Alexander Island. (*In* ADIE, R. J. *ed. Antarctic geology*. Amsterdam, North-Holland Publishing Company, 53–64.)

KIRCHNER, J. F. *and* BENTLEY, C. R. 1979. Seismic short-refraction studies on the Ross Ice Shelf, Antarctica. *Journal of Glaciology*, **24** (90), 313–19.

KOHNEN, H. 1971. The relation between seismic firn structure, temperature and accumulation. *Zeitschrift für Gletscherkunde und Glacialgeologie*, **7** (1–2), 141–51.

KOHNEN, H. 1972. Über die Beziehung zwischen seismischen Geschwindigkeiten und der Dichte in Firn und Eis. *Zeitschrift für Geophysik*, **38** (5), 925–35.

KOHNEN, H. 1974. The temperature dependence of seismic waves in ice. *Journal of Glaciology*, **13** (6), 144–7.

MASOLOV, V. N., KURININ, R. G. *and* GRIKUROV, G. E. 1980. Crustal structures and tectonic significance of Antarctic rift zones (from geophysical evidence). (*In* CRESSWELL, M. M. *and* VELLA, P. *eds. Gondwana five. Selected papers and abstracts presented at the Fifth International Gondwana Symposium*. A. A. Balkema/Rotterdam, 303–9.

RENNER, R. G. B., STURGEON, L. J. S. *and* GARRETT, S. W. 1985. Reconnaissance gravity and aeromagnetic surveys of the Antarctic Peninsula. *British Antarctic Survey Scientific Reports* No. 110.

SLICHTER, L. B. 1932. The theory of the interpretation of seismic travel–time curves in horizontal structures. *Physics*, **3**, 273–95.

STOREY, B. C. *and* GARRETT, S. W. 1985. Crustal growth of the Antarctic Peninsula by accretion, magmatism and extension. *Geological Magazine*, **122**, 5–14.

TAYLOR, G. K. *and* SHAW, J. 1985. Preliminary palaeomagnetic results from Alexander Island, Antarctica. *Geophysical Journal of the Royal Astronomical Society*, **81** (1), Abstract, p. 324.

VANNEY, J. R. *and* JOHNSON, G. L. 1976. Geomorphology of the Pacific Continental Margin of the Antarctic Peninsula. (*In* HOLLISTER, C. D. *and* CRADDOCK, C. *eds. Initial Report Deep Sea Drilling Project*, 35. U.S. Government Printing Office, Washington, D.C.)